

Research Article

A Mathematical Model for Controlling SARS-COV 2 by Triplet Oxygen Molecules, Spinning Bubbles and Other Spinors

Massimo Fioranelli^{1*}, Phoka C. Rathebe², Alireza Sepehri³, Hijaz Ahmad^{4,5,6}, Aroonkumar Beesham⁷, Alireza Haghpeima⁸

¹Department of Human Sciences, Guglielmo Marconi University, Via Plinio 44, 00193 Rome, Italy

²Department of Environmental Health, Faculty of Health Sciences, Doornfontein Campus, University of Johannesburg, P.O. Box 524, Johannesburg 2006, South Africa

³Instituto Terapie Sistemiche Integrate, Via di Trasono, 00199 Rome, Italy

⁴Near East University, Operational Research Center in Healthcare, TRNC Mersin 10, Nicosia 99138, Turkey

⁵Department of Mathematics, College of Science, Korea University, 145 Anam-ro, Seongbuk-gu, Seoul 02841, South Korea

⁶Department of Technical Sciences, Western Caspian University, Baku 1001, Azerbaijan

⁷Faculty of Natural Sciences, Mangosuthu University of Technology, Umlazi, South Africa

⁸Department of Physics, Mashhad branch, Islamic Azad University, Mashhad, Iran
E-mail: m.fioranelli73@gmail.com

Received: 14 September 2023; **Revised:** 21 October 2023; **Accepted:** 26 October 2023

Abstract: Background: One of best ways to repel harmful viruses like corona is using of repulsive force between spinors which are existed within structures of cells and viruses. These spins could be induced within virus and cell structures by external magnetic fields which are emitted from currents of ions within blood cells. Motions of charges and ions within blood vessels produces magnetic fields. These fields force on spinors within cell and virus structures within alveolus and make them parallel. These spinning viruses interact with triplet spins of oxygen molecules within alveolus. According to the Pauli exclusion principle, parallel spinors repel each other and anti parallel spinors attract each other. Thus the triplet state of spinors of oxygen molecules could help cells to repel viruses with the same induced spin states. On the other hand, by using external waves, one can induce virtual viruses with opposite induced spins within alveolus and cancel effects of real viruses. We use of this property in controlling viral diseases. Purpose: Our aim is to 1. propose a mathematical model which use of repulsive force between parallel spinors and attractive force between anti parallel spinors within structures of oxygen molecules; alveolar cells and viruses to control COVID-19 disease. 2. We also introduce a mechanism mathematically to induce virtual viruses with opposite spinor states around real viruses within alveolus. These virtual viruses cancel effects of real viruses and form harmless bubbles. 3. We introduce a quantum mask to use of spinor interactions and repel viruses. Method: In this model, hemoglobin molecules and their irons, take special spins from heart waves, move along vessels and induce them to spinors within the structure of other cells like alveolar ones. These spinors select oxygen triplet molecules with opposite spins and repel parallel spin ones. Also, spinors which form RNAs and proteins of viruses could take parallel or opposite spins of any external magnetic field. These spinning viral structures are attracted by opposite spinors of alveolar cells and repel the oxygen molecules with parallel spins. This causes to a decrease

in number of needed oxygen molecules within human's body. To control these viruses, we build a system which includes:

1. A vessel of water and oxygen molecules which be located near the face and is open.
2. A vessel of viruses which is located far from the face and is closed.
3. A heater-cooler system which connects two vessels.

Results: During the respiration, alveolar air molecules go out, collide with vessels, attract oxygen and viral molecules with opposite spins and repel parallel ones. Consequently, viruses which could be attracted by alveolar cells go away from the face and build a mask against any similar spinning virus in another end of system. On the other hand, spinors around the viruses in second and closed vessel which couldn't be attracted by alveolar cells, form some bubbles. By heating and cooling the system these bubble shapes are induced in open vessel of system, make virtual viruses and bubbles which fly towards the face and alveolus. These virtual viruses attract real viruses and make spin-less bubbles which are harmless and go out of human's body. We formulate the model and obtain related currents. Conclusion: By using repulsive forces between triplet oxygen states and spinors within viral structures and induction of virtual viruses with opposite spins around real viruses; harmful effects of these viruses could be cancelled. Because; spinors of viruses are surrounded by anti parallel spinors of oxygen molecules and virtual viruses and harmless bubbles and pairs are formed. We have formulate the mechanism and obtained frequencies of waves which induce virtual viruses within alveolus.

Keywords: spinning virus, spinor mask, alveolus, bubbles, triplet oxygen molecules

MSC: 65L05, 34K06, 34K28

1. Introduction

In last decades, human confronts with wonderful diseases like different types of cancers and viruses. Although, technology helps to cure many of these diseases; however, it seems that some of them need to more progress in medical knowledge. For example, to prevent of spreading microbial diseases, some vaccines have been introduced and some drugs have been suggested. However, some of these medical methods are expensive specially for non-developing countries and providing and buying vaccines and drugs are very hard. For this reason, we should find some more simplest methods to cure and control these diseases. One of main diseases which all try to find cheapest medical methods for its curing is coronavirus disease 2019 (COVID-19). This diseases is emerged by severe acute respiratory syndrome coronavirus 2 (SARS-CoV-2). The first known case was identified in Wuhan, China, in December 2019. Then, it has spread worldwide and cause to an ongoing pandemic [1–4]. Recently, several types of vaccines have been proposed which companies claiming their good actions against SARS-CoV-2. Some COVID-19 vaccines like the Pfizer-BioNTech and Moderna vaccines have been designed to apply RNA for stimulating the immune responses. When introduced into human tissue, the vaccine contains either self-replicating RNA or messenger RNA (mRNA), which both cause cells to express the SARS-CoV-2 spike protein. This teaches the body how to identify and destroy the corresponding pathogen [5–7]. Some other types of vaccines like the Sputnik V COVID-19 vaccine use an adenovirus shell containing DNA that encodes a SARS-CoV-2 protein. The viral vector-based vaccines against COVID-19 are non-replicating, meaning that they do not make new virus particles, but rather produce only the antigen which elicits a systemic immune response [8]. Also, there are some inactivated vaccines which consist of virus particles. These particles are grown in culture and then killed using a method such as heat or formaldehyde to lose disease producing capacity, while still stimulating an immune response [9]. Besides vaccines, some drugs have suggested which may be helpful in curing COVID-19 disease. For example, some antiviral medications like Molnupiravir inhibit the replication of certain RNA viruses, and are used to treat COVID-19 in those infected by SARS-CoV-2 [10]. Or some drugs like Nirmatrelvir which is an antiviral medication developed by Pfizer and act as 3CL protease inhibitor [11]. And also some drugs use of antibodies against SARS-COV-2 [12]. Some of these drugs are expensive and many people couldn't provide them easily. For this reason, we should explore more better medical cures. To this aim, we can use of some physical concepts in controlling viruses [13, 14]. Specially in the case of SARS-COV-2, there are some hopes which they use of spinor waves in exchanging information. For example, it seems that by entering these viruses into alveolus, triplet oxygen molecules go out from alveolar space. Maybe, these viruses

produce some spinor states which repel parallel states like triplet states of oxygen molecules. If this hypothesis be true, we can use of quantum principles in controlling COVID-19 disease.

Up to date; some mathematical models for spreading of COVID-19 virus and also its interactions with cells have been proposed. For example, a paper considered the SARS-CoV-2 virus by using a system of equations. This model could generate numerical results to predict the outcome of virus spreadings all over India [15]. Another group proposed and analysed a mathematical model for the dynamics of COVID-19 transmission influenced by awareness campaigns through social media [16]. In most of models, complicated mathematical equations have been applied [17–19]. In another article, authors evaluated and predicted the transmission dynamics of deadly viruses like COVID-19 [20]. In other study, a COVID-19 dynamical transmission model of a coupled non-linear fractional differential equation in the Atangana-Baleanu Caputo sense was proposed [21]. All of these researches show that math could help us to propose good models in COVID-19 related subjects.

In previous works, some mathematical models have been proposed to show the growth rate or spreading velocity of COVID-19. Also, some researches focus on action mechanism of virus and biological interactions between viruses and cells. In this research, we use of quantum properties of spinors within the structures of cells, oxygen molecules and viruses to control viral diseases. According to Pauli exclusion principle, parallel spinors repel each other. Also, anti parallel spinors attract each other. Thus, we have two ways. 1. We could use of triplet states of oxygen molecules to repel viruses which have parallel spinors within their structures. 2. We could induce virtual viruses with opposite spins around real viruses to become pair with them and cancel their effects.

The outline of paper is as follows: In Section 2, we describe the model and design some spinor curing methods and spinor masks against COVID-19. In Section 3, we will do related calculations and propose mathematical results.

2. The model: Spinor curing methods and spinor masks against SARS-COV 2

In this section, we suggest a model for controlling spinning viruses by using spinning biological molecules like triplet oxygen molecules or viruses with opposite spins. In this model:

1. We use of this fact that parallel spins repel each other and anti-parallel spins attract each other. The velocity of exchanging information between spins is more than the velocity of light. For example, in a pair of two anti-parallel spins, when the arrow of one spin changes, the arrow of their spin could change immediately (See Figure 1).

2. It has been known that the stable spinor state of an oxygen molecule (O-O) is a triplet. A triplet oxygen includes at least two parallel spinors like two parallel electrons.

3. Triple oxygen molecules (O-O($\uparrow\uparrow$)) could attract triplet oxygen molecules with opposite directions ((O-O($\downarrow\downarrow$))). Also these molecules repel oxygen molecules with the same spins (O-O($\uparrow\uparrow$)) (See Figure 1).

4. Within each alveolus of lung, there are several types of cells like AT I which help in exchanging oxygen and carbon gases with blood cells and also AT II and macrophages which have different actions (See Figure 2).

5. Around each alveolus, there are some blood vessels which red blood cells including hemoglobin move along them (See Figure 2).

6. Hemoglobin contains iron atoms and could take spinning states and induce them to spinors within alveolar cells and ions around them (See Figure 2). Because, the cellular membranes, DNAs and other biological structures within the alveolar cells are built from spinors like electrons and atoms and could have spins.

7. Spinning structures around or within alveolar cells could attract only one type of oxygen molecules with opposite spins and repel spinning molecules with parallel spins (See Figure 2).

8. Viruses also have RNAs, proteins and membranes which are built from spinors like electrons and atoms. These structures could take a special spin in an external magnetic field.

9. Alveolar cells could attract spinning viruses with opposite spins. Spins of these viruses are in parallel with spins of oxygen molecules and consequently repel them. This causes that needed oxygen molecules within an alveolus decrease (See Figure 3).

10. To cure spinning viral diseases, we provide two vessels, one including water molecules and oxygen gases and other including spinning viruses (See Figure 4).

11. We put two vessels near each other and connect them to a heater-cooler system. Two ends of vessels should be warm and middle of them should be cooled (See Figure 4).

12. We bring this system near the face of patients. Spinning oxygen molecules collide with vessels and induce reverse spins to water and oxygen molecules within vessels (See Figure 4).

13. Spinning viruses with opposite spins become closed and other viruses with the same spins go away (See Figure 4).

14. By changing temperature along vessels, spinors move, build some bubbles and take the shape of viruses. Consequently, within the open water vessel, these bubbles are induced and some virtual viruses are emerged. Spins of these viruses are in opposite with spins of real viruses within person's body (See Figure 4).

15. Virtual viruses are confined within water bubbles and eventually evaporate and enter into the body and alveolus (See Figure 4).

16. Virtual viruses combine with real viruses with opposite spins and form some spinless bubbles. These bubbles have no effect on cells and go out of alveolus (See Figure 4).

17. This method could be used in designing some spinor masks. We can provide a system from combinations of oxygen molecules and spinning viruses (See Figure 5).

18. During respirations, spinning oxygen molecules go out and interact with molecules within this system. Biological molecules with opposite spins become closed to the face and other molecules go away (See Figure 5).

19. When spinning viruses which could be selected by alveolar cells become closed to this mask, confront with similar spins and go away. Thus, this mask repels any harmful spinning virus (See Figure 5).

20. On the other hand, interactions between parallel spins cause that spins of oxygen molecules near the face reverse and move towards it. This means that needed oxygen or respiration could be provided (See Figure 5).

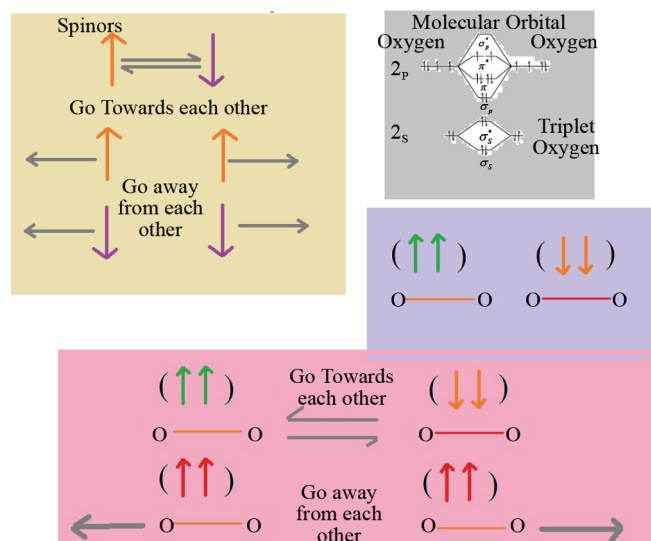


Figure 1. Triplet oxygen molecules repel molecules and spinors with the same spins and attract molecules and spinors with opposite spins

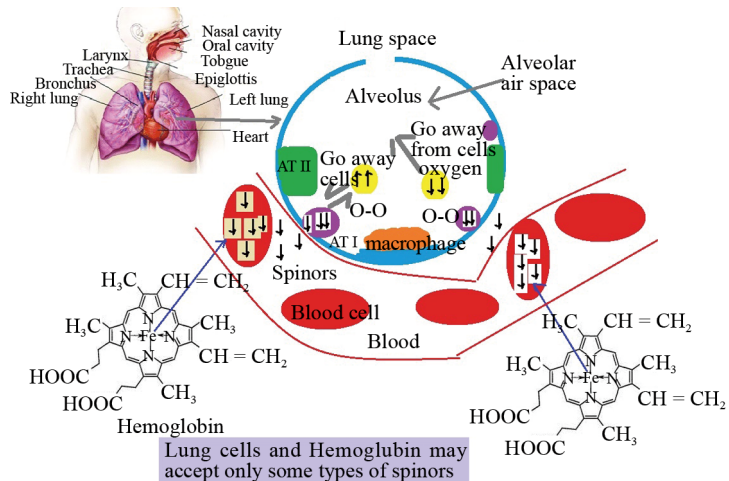


Figure 2. Hemoglobin induces special spins on cellular membranes and spinors around them within an alveolus. These spinning cells choose oxygen molecules with opposite spins

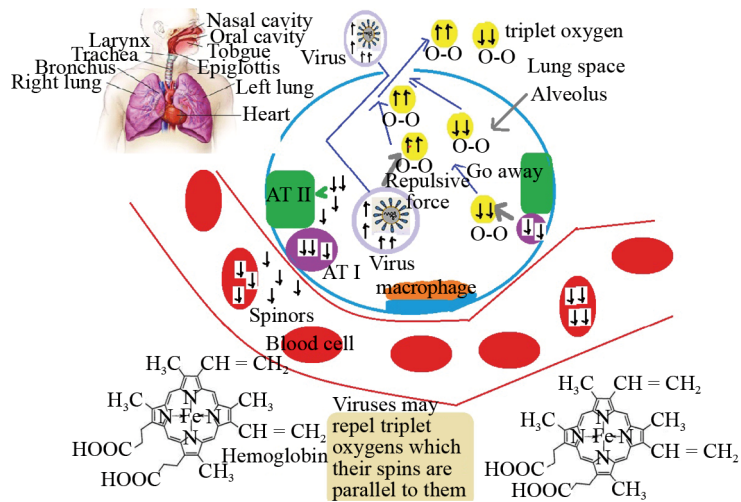


Figure 3. Viruses with opposite spins respect to cells could be attracted by them. Also, these viruses repel all oxygen molecules with the same spins

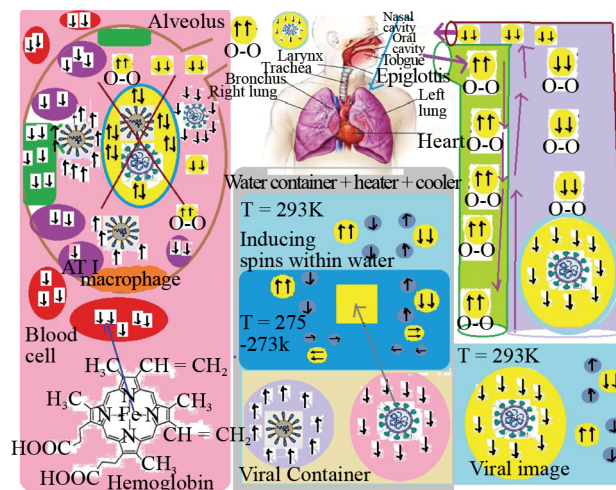


Figure 4. A model for inducing virtual viruses around cells within alveolus to combine with real viruses with opposite spins and cancel their effects

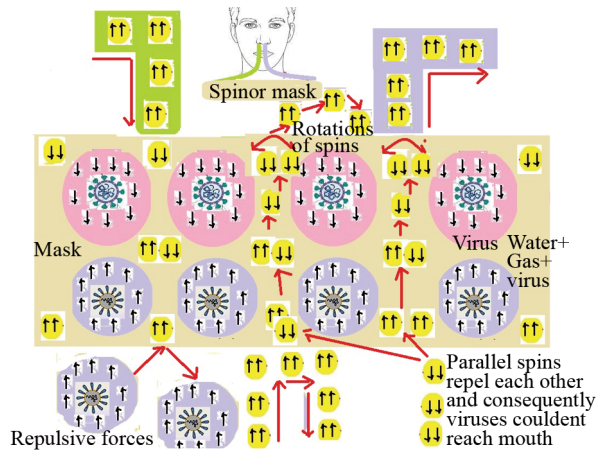


Figure 5. A model for spinor mask which could be built by viruses, water and spinning oxygen molecules

3. The mathematical results

In this section, we formulate the model and obtain the current of bubbles and oxygen molecules which emit needed waves for inducing virtual viruses around real viruses within lung. These virtual particles cancel the real viral effects and control viral diseases. To begin discussion, we suppose that each steam plane of bubbles has a total spin. Each steam plane is formed from several numbers of sheets. Total spin of a steam system could be obtained from below equation:

$$S_{Steam} \rightarrow \sum_j n_{sheet, j} S_{sheet, j} \quad (1)$$

where S_{Steam} is total spin of a steam system, $n_{sheet, j}$ is the number of sheets, j is the number of sheets and $S_{sheet, j}$ is the spin of sheets. Spin of each sheet could be obtained from below equation:

$$S_{sheet, j} \rightarrow \sum_i n_{bubble, ij} S_{bubble, ij} \quad (2)$$

where $n_{bubble, ij}$ is the number of bubbles, $S_{bubble, ij}$ is the spin of bubbles and i, j are related indices. Each bubble can contain several gas molecules like triplet O_2 . Thus, total spin of a bubble molecule could be obtained from below equation:

$$S_{bubble, ij} \rightarrow \sum_k n_{\uparrow\uparrow, ijk} S_{\uparrow\uparrow, ijk} + \sum_l n_{\downarrow\downarrow, ijl} S_{\downarrow\downarrow, ijl} \quad (3)$$

where $n_{\uparrow\uparrow, ijk}$ and $n_{\downarrow\downarrow, ijl}$ are number of free electrons and holes. Also, ijk are related indices and $S_{\uparrow\uparrow, ijk}$ and $S_{\downarrow\downarrow, ijl}$ are spins of free electrons and holes. Substituting results of Equations (2) and (3) in Equation (1) gives:

$$S_{Steam} \rightarrow \sum_j n_{sheet, j} \sum_i n_{bubble, ij} [\sum_k n_{\uparrow\uparrow, ijk} S_{\uparrow\uparrow, ijk} + \sum_l n_{\downarrow\downarrow, ijl} S_{\downarrow\downarrow, ijl}] \quad (4)$$

Using above result, we can obtain the below energy density:

$$U_{Steam} \rightarrow \frac{[\hbar \mathcal{N}' S_{Steam}]^2}{2\mu_0}$$

$$\mathcal{N}' \rightarrow \frac{e}{2m\hbar} (e, m, \hbar, c \dots) \quad (5)$$

where \hbar is the plank constant, S_{Steam} is the steam spin, μ_0 is the magnetic constant and \mathcal{N}' is a constant depending on mass and electric charges. Substituting energy density of Equation (4) in Equation (5) gives:

$$U_{Steam} \rightarrow \frac{[\hbar \mathcal{N}']^2}{2\mu_0} [\sum_j n_{sheet, j} \sum_i n_{bubble, ij} [\sum_k n_{\uparrow\uparrow, ijk} S_{\uparrow\uparrow, ijk} + \sum_l n_{\downarrow\downarrow, ijl} S_{\downarrow\downarrow, ijl}]]^2 \quad (6)$$

Using above energy density, we can obtain total energy of a steam:

$$E_{Steam} = U_{Steam} V_{Steam} \quad (7)$$

where V_{Steam} is the volume of a steam system and could be obtained from below equation:

$$V_{Steam} = 2\pi [\sum_j n_{sheet, j} \sum_i n_{bubble, ij} [R_{bubble, ij} + x]] [\sum_j n_{sheet, j} [L_{sheet-sheet, j} + x]] \quad (8)$$

where $L_{sheet-sheet, j}$ is the steam sheet length, x is the size of vibration and $R_{bubble, ij}$ is the radius of bubble molecule. Substituting results of Equations (6) and (8) in Equation (7) gives:

$$E_{Steam} \rightarrow \frac{\mathcal{N}' [\hbar]^2}{2\mu_0} [\sum_j n_{sheet, j} \sum_i n_{bubble, ij} [\sum_k n_{\uparrow\uparrow, ijk} S_{\uparrow\uparrow, ijk} + \sum_l n_{\downarrow\downarrow, ijl} S_{\downarrow\downarrow, ijl}]]^2$$

$$\odot 2\pi [\sum_j n_{sheet, j} \sum_i n_{bubble, ij} [R_{bubble, ij} + x]] [\sum_j n_{sheet, j} [L_{sheet-sheet, j} + x]] \quad (9)$$

Above equation corresponds to two coupled sheets. However, by separating two sheets, some extra spinors could enter into this system and produce some noises in entangled paired. For example, suppose that we have two entangled spinors at first:

$$|\uparrow\uparrow\rangle \text{ or } |\downarrow\downarrow\rangle \quad (10)$$

Then, each of these spinors could produce several thermal entanglements with extra spinors in medium [13, 14]:

$$\begin{aligned}
|\uparrow\uparrow, initial\rangle &\rightarrow [\cos\alpha\Sigma_{n=0, 1} \tan^n \alpha |\uparrow, n\rangle_{+1} |\downarrow, n\rangle_{-1}] \\
[\cos\beta\Sigma_{m=0, 1} \tan^m \beta |\uparrow, m\rangle_{+1} |\downarrow, m\rangle_{-1}] &
\end{aligned} \tag{11}$$

where

$$\begin{aligned}
\tan \alpha &\approx \exp\left(-\frac{\pi E_{\text{noise, spinor-entanglement, } \uparrow}}{T_{\text{spinor-entanglement, } \uparrow}}\right) \\
\tan \beta &\approx \exp\left(-\frac{\pi E_{\text{noise, spinor-entanglement, } \downarrow}}{T_{\text{spinor-entanglement, } \downarrow}}\right)
\end{aligned} \tag{12}$$

And

$$E_{\text{noise, spinor-entanglement}} \rightarrow \frac{[\hbar]^2 S_{\text{noise, spin1}} S_{\text{noise, spin2}}}{2\mu_0} \tag{13}$$

Substituting results of Equation (11) in Equation (9) yields:

$$\begin{aligned}
E_{\text{Steam}} &\rightarrow \frac{[\mathcal{N}'\hbar]^2}{2\mu_0} [\Sigma_j n_{\text{sheet}, j} \Sigma_i n_{\text{bubble}, ij} [\Sigma_k n_{\uparrow\uparrow, ijk} S_{\uparrow\uparrow, ijk} + \Sigma_l n_{\downarrow\downarrow, ijl} S_{\downarrow\downarrow, ijl}]] \\
&\odot \left[\prod_{z=1\dots n} \cos \alpha_{1, \text{noise}} \dots \cos \alpha_{w, \text{noise}} \right] \times \odot [\Sigma_{f=0, 1} \tan^{f_1} \alpha_{1, \text{noise}}] \dots [\Sigma_{f=0, 1} \tan^f \alpha_{w, \text{noise}}] \\
&\frac{\odot \mathcal{N}'[\hbar]^2}{2\mu_0} [\Sigma_m n_{\text{sheet}, m} \Sigma_n n_{\text{bubble}, mn} [\Sigma_x n_{\uparrow\uparrow, mx} S'_{\uparrow\uparrow, mx} + \Sigma_y n_{\downarrow\downarrow, my} S'_{\downarrow\downarrow, my}]] \\
&\odot [2\pi [\Sigma_j n_{\text{sheet}, j} \Sigma_i n_{\text{bubble}, ij} [R_{\text{bubble}, ij} + x]] [\Sigma_j n_{\text{sheet}, j} [L_{\text{sheet-sheet}, j} + x]] \\
&+ 2\pi [\Sigma_m n_{\text{sheet}, m} \Sigma_i n_{\text{bubble}, nm} [R'_{\text{bubble}, nm} + x]] [\Sigma_m n_{\text{sheet}, m} [L'_{\text{sheet-sheet}, n} + x]] \odot H_{\text{Separation Distance}} \tag{14}
\end{aligned}$$

where $H_{\text{Separation Distance}}$ is the Separation Distance between coupled steam sheets. By taking derivative of above equation with respect to x , one obtains:

$$F_{\text{Steam}} = \frac{d E_{\text{Steam}}}{X} = K_{\text{Steam}} x + \text{constant} \tag{15}$$

where

$$\begin{aligned}
K_{Steam} = & [2\pi[\sum_j n_{sheet, j} \sum_i n_{bubble, ij}] [\sum_j n_{sheet, j}] + 2\pi[\sum_m n_{sheet, m} \sum_i n_{bubble, nm}] [\sum_m n_{sheet, m}]] \\
& \odot \frac{[\mathcal{N}'\hbar]^2}{2\mu_0} [\sum_j n_{sheet, j} \sum_i n_{bubble, ij} [\sum_k n_{\uparrow\uparrow, ijk} S_{\uparrow\uparrow, ijk} + \sum_l n_{\downarrow\downarrow, ijl} S_{\downarrow\downarrow, ijl}]] \\
& \odot \left[\prod_{z=1 \dots n} \cos \alpha_{1, noise} \dots \cos \alpha_{w, noise} \right] \times \\
& \odot [\sum_{f_1=0, 1} \tan^{f_1} \alpha_{1, noise}] \dots [\sum_{f_w=0, 1} \tan^{f_w} \alpha_{w, noise}] \\
& \odot \frac{[\mathcal{N}'\hbar]^2}{2\mu_0} [\sum_m n_{sheet, m} \sum_n n_{bubble, mn} [\sum_x n_{\uparrow\uparrow, mnx} S'_{\uparrow\uparrow, mnx} + \sum_y n_{\downarrow\downarrow, mny} S'_{\downarrow\downarrow, mny}]] \odot H_{Separation Distance} \quad (16)
\end{aligned}$$

For above equations, frequencies could be obtained from below equations.

$$\begin{aligned}
V_{Exchanged\ wave, sheet} = & \frac{1}{2\pi} \left[\frac{K_{Steam}}{M_{electron}} \right]^{\frac{1}{2}} \rightarrow \frac{1}{2\pi} \left[\frac{1}{M_{Tot, electron}} \right]^{\frac{1}{2}} [[2\pi[\sum_j n_{sheet, j} \sum_i n_{bubble, ij}] [\sum_j n_{sheet, j}]] \\
& + 2\pi[\sum_m n_{sheet, m} \sum_i n_{bubble, nm}] [\sum_m n_{sheet, m}]] \\
& \odot \frac{[\mathcal{N}'\hbar]^2}{2\mu_0} [\sum_j n_{sheet, j} \sum_i n_{bubble, ij} [\sum_k n_{\uparrow\uparrow, ijk} S_{\uparrow\uparrow, ijk} + \sum_l n_{\downarrow\downarrow, ijl} S_{\downarrow\downarrow, ijl}]] \\
& \odot \left[\prod_{z=1 \dots n} \cos \alpha_{1, noise} \dots \cos \alpha_{w, noise} \right] \times \odot [\sum_{f_1=0, 1} \tan^{f_1} \alpha_{1, noise}] \dots [\sum_{f_w=0, 1} \tan^{f_w} \alpha_{w, noise}] \\
& \odot \frac{[\mathcal{N}'\hbar]^2}{2\mu_0} [\sum_m n_{sheet, m} \sum_n n_{bubble, mn} [\sum_x n_{\uparrow\uparrow, mnx} S'_{\uparrow\uparrow, mnx} + \sum_y n_{\downarrow\downarrow, mny} S'_{\downarrow\downarrow, mny}]] \\
& \odot H_{Separation Distance}]^{1/2} \quad (17)
\end{aligned}$$

where

$$\begin{aligned}
M_{Tot, electron} \rightarrow & [\sum_j n_{sheet, j} \sum_i n_{bubble, ij} [\sum_k n_{\uparrow\uparrow, ijk} m_{\uparrow\uparrow, ijk} + \sum_l n_{\downarrow\downarrow, ijl} m_{\downarrow\downarrow, ijl}]] \\
& + [\sum_m n_{sheet, m} \sum_n n_{bubble, mn} [\sum_x n_{\uparrow\uparrow, mnx} m'_{\uparrow\uparrow, mnx} + \sum_y n_{\downarrow\downarrow, mny} m'_{\downarrow\downarrow, mny}]] + m_{noise} \quad (18)
\end{aligned}$$

Substituting result of Equation (18) in Equation (17) yields:

$$\begin{aligned}
V_{\text{Exchanged wave, sheet}} &= \frac{1}{2\pi} \left[\frac{K_{\text{Steam}}}{M_{\text{electron}}} \right]^{\frac{1}{2}} \rightarrow \frac{1}{2\pi} \odot \left[[\Sigma_j n_{\text{sheet}}, j\Sigma_i n_{\text{bubble}}, ij] [\Sigma_k n_{\uparrow\uparrow}, ijk m'_{\uparrow\uparrow, ijk} + \Sigma_l n_{\downarrow\downarrow}, ijl m'_{\downarrow\downarrow, ijl}] \right. \\
&+ [\Sigma_m n_{\text{sheet}}, m\Sigma_n n_{\text{bubble}}, mn] [\Sigma_x n_{\uparrow\uparrow}, mnx m'_{\uparrow\uparrow, mnx} + \Sigma_y n_{\downarrow\downarrow}, mny m'_{\downarrow\downarrow, mny}] + m_{\text{noise}} \left. \right]^{\frac{-1}{2}} \\
&\odot \left[[2\pi [\Sigma_j n_{\text{sheet}}, j\Sigma_i n_{\text{bubble}}, ij] [\Sigma_j n_{\text{sheet}}, j] + 2\pi [\Sigma_m n_{\text{sheet}}, m\Sigma_i n_{\text{bubble}}, nm] [\Sigma_m n_{\text{sheet}}, m]] \right. \\
&\frac{\odot [\mathcal{N}'\hbar]^2}{2\mu_0} [\Sigma_j n_{\text{sheet}}, j\Sigma_i n_{\text{bubble}}, ij] [\Sigma_k n_{\uparrow\uparrow}, ijk S'_{\uparrow\uparrow, ijk} + \Sigma_l n_{\downarrow\downarrow}, ijl S'_{\downarrow\downarrow, ijl}] \\
&\odot \left[\prod_{z=1\dots n} \cos \alpha_{1, \text{noise}} \dots \cos \alpha_{w, \text{noise}} \right] \times \odot [\Sigma_{f_1=0, 1} \tan^{f_1} \alpha_{1, \text{noise}}] \dots [\Sigma_{f=0, 1} \tan^f \alpha_{w, \text{noise}}] \\
&\frac{\odot [\mathcal{N}'\hbar]^2}{2\mu_0} [\Sigma_m n_{\text{sheet}}, m\Sigma_n n_{\text{bubble}}, mn] [\Sigma_x n_{\uparrow\uparrow}, mnx S'_{\uparrow\uparrow, mnx} + \Sigma_y n_{\downarrow\downarrow}, mny S'_{\downarrow\downarrow, mny}] \\
&\odot H_{\text{Separation Distance}}]^{1/2} \tag{19}
\end{aligned}$$

Above frequency corresponds to Exchanged waves between steam sheets. However, it ignores the role of radiated spinors from biological cells. A cell could emit some spinors which fill holes or produce some new holes within steam system. For a normal cell, we can write the below frequency:

$$\begin{aligned}
V_{\text{Exchanged wave, sheet, normal cell}} &= \frac{1}{2\pi} \left[\frac{K_{\text{Steam}}}{M_{\text{electron}}} \right]^{\frac{1}{2}} \rightarrow \frac{1}{2\pi} \\
&\odot \left[[\Sigma_j n_{\text{sheet}}, j\Sigma_i n_{\text{bubble}}, ij] [\Sigma_k n_{\uparrow\uparrow}, ijk [m'_{\uparrow\uparrow, ijk} - m_{\text{radiated}(\uparrow\uparrow), \text{normal cell}, ijk}] \right. \\
&+ \Sigma_l n_{\downarrow\downarrow}, ijl [m'_{\downarrow\downarrow, ijl} - m_{\text{radiated}(\downarrow\downarrow), \text{normal cell}, ijl}]] \\
&+ [\Sigma_m n_{\text{sheet}}, m\Sigma_n n_{\text{bubble}}, mn] [\Sigma_x n_{\uparrow\uparrow}, mnx [m'_{\uparrow\uparrow, mnx} - m'_{\text{radiated}(\uparrow\uparrow), \text{normal cell}, mnx}] \\
&+ \Sigma_y n_{\downarrow\downarrow}, mny [m'_{\downarrow\downarrow, mny} - m'_{\text{radiated}(\downarrow\downarrow), \text{normal cell}, mny}]] + m_{\text{noise}} \left. \right]^{\frac{-1}{2}} \\
&\odot \left[[2\pi [\Sigma_j n_{\text{sheet}}, j\Sigma_i n_{\text{bubble}}, ij] [\Sigma_j n_{\text{sheet}}, j] \right. \\
&+ 2\pi [\Sigma_m n_{\text{sheet}}, m\Sigma_i n_{\text{bubble}}, nm] [\Sigma_m n_{\text{sheet}}, m]]
\end{aligned}$$

$$\begin{aligned}
& \odot \frac{[\mathcal{N}'\hbar]^2}{2\mu_0} [\Sigma_j n_{sheet, j} \Sigma_i n_{bubble, ij} [\Sigma_k [n_{\uparrow\uparrow, ijk} S_{\uparrow\uparrow, ijk} \\
& - n_{radiated}(\uparrow\uparrow), normal\ cell, ijk] S_{radiated}(\uparrow\uparrow), normal\ cell, ijk] \\
& + \Sigma_l [n_{\downarrow\downarrow, ijl} S_{\downarrow\downarrow, ijl} - n_{radiated}(\downarrow\downarrow), normal\ cell, ijl] S_{radiated}(\downarrow\downarrow), normal\ cell, ijl]] \\
& \odot \left[\prod_{z=1..n} \cos \alpha_{1, noise} \dots \cos \alpha_{w, noise} \right] \times \odot [\Sigma_{f_1=0, 1} \tan^{f_1} \alpha_{1, noise}] \dots [\Sigma_{f=0, 1} \tan^f \alpha_{w, noise}] \\
& \odot \frac{[\mathcal{N}'\hbar]^2}{2\mu_0} [\Sigma_m n_{sheet, m} \Sigma_n n_{bubble, mn} \odot [\Sigma_x [n_{\uparrow\uparrow, mnx} S'_{\uparrow\uparrow, mnx} \\
& - n_{radiated}(\uparrow\uparrow), normal\ cell, mnx] S'_{radiated}(\uparrow\uparrow), normal\ cell, mnx] \\
& + \Sigma_y [n_{\downarrow\downarrow, mny} S'_{\downarrow\downarrow, mny} - n_{radiated}(\downarrow\downarrow), normal\ cell, mny] S'_{radiated}(\downarrow\downarrow), normal\ cell, mny]] \\
& \odot [H_{Separation\ Distance}]^{1/2} \tag{20}
\end{aligned}$$

Above frequency corresponds to Exchanged waves between two sheets, one coming from interior of human's body near the human cells within lung and other coming from water exterior it. According to observations, viruses cause that cells emit different numbers of spinors and holes and radiated waves have below frequency:

$$\begin{aligned}
\mathbf{V}_{Exchanged\ wave, sheet, (virus-cell)} &= \frac{1}{2\pi} \left[\frac{K_{Steam}}{M_{electron}} \right]^{\frac{1}{2}} \rightarrow \frac{1}{2\pi} \\
& \odot [[\Sigma_j n_{sheet, j} \Sigma_i n_{bubble, ij} [\Sigma_k n_{\uparrow\uparrow, ijk} [m_{\uparrow\uparrow, ijk} - m_{radiated}(\uparrow\uparrow), (virus-cell), ijk] \\
& + \Sigma_l n_{\downarrow\downarrow, ijl} [m_{\downarrow\downarrow, ijl} - m_{radiated}(\downarrow\downarrow), (virus-cell), ijl]] \\
& + [\Sigma_m n_{sheet, m} \Sigma_n n_{bubble, mn} [\Sigma_x n_{\uparrow\uparrow, mnx} [m'_{\uparrow\uparrow, mnx} - m'_{radiated}(\uparrow\uparrow), (virus-cell), mnx] \\
& + \Sigma_y n_{\downarrow\downarrow, mny} [m'_{\downarrow\downarrow, mny} - m'_{radiated}(\downarrow\downarrow), (virus-cell), mny]]] + m_{noise}]^{\frac{-1}{2}} \\
& \odot [[2\pi [\Sigma_j n_{sheet, j} \Sigma_i n_{bubble, ij}] [\Sigma_j n_{sheet, j}] + 2\pi [\Sigma_m n_{sheet, m} \Sigma_i n_{bubble, nm}] [\Sigma_m n_{sheet, m}]]
\end{aligned}$$

$$\begin{aligned}
& \frac{\odot [\mathcal{N}'\hbar]^2}{2\mu_0} [\Sigma_j n_{sheet, j} \Sigma_i n_{bubble, ij} [\Sigma_k [n_{\uparrow\uparrow, ijk} S_{\uparrow\uparrow, ijk} \\
& - n_{radiated}(\uparrow\uparrow), (virus-cell), ijk] S_{radiated}(\uparrow\uparrow), (virus-cell), ijk] \\
& + \Sigma_l [n_{\downarrow\downarrow, ijl} S_{\downarrow\downarrow, ijl} - n_{radiated}(\downarrow\downarrow), (virus-cell), ijl] S_{radiated}(\downarrow\downarrow), (virus-cell), ijl]] \\
& + \Sigma_y [n_{\downarrow\downarrow, mny} S'_{\downarrow\downarrow, mny} - n_{radiated}(\downarrow\downarrow), (virus-cell), mny] S'_{radiated}(\downarrow\downarrow), (virus-cell), mny]] \\
& \odot H_{Separation\ Distance}^{1/2} \odot \left[\prod_{z=1\dots n} \cos \alpha_{1, noise} \dots \cos \alpha_{w, noise} \right] \times \\
& \odot [\Sigma_{f_1=0, 1} \tan^{f_1} \alpha_{1, noise}] \dots [\Sigma_{f=0, 1} \tan^f \alpha_{w, noise}] \frac{\odot [\mathcal{N}'\hbar]^2}{2\mu_0} [\Sigma_m n_{sheet, m} \Sigma_n n_{bubble, mn} \\
& \odot [\Sigma_x [n_{\uparrow\uparrow, mnx} S'_{\uparrow\uparrow, mnx} - n_{radiated}(\uparrow\uparrow), (virus-cell), mnx] S'_{radiated}(\uparrow\uparrow), (virus-cell), mnx] \tag{21}
\end{aligned}$$

Comparing Equations (20) and (21), we find that (virus-cell)s emit waves with different frequencies with respect to normal cells. Thus, by considering Exchanged waves between steam sheets, one can diagnose (virus-cell)s.

Now, the question arises that how we can induce virtual viruses around a cell? To answer this question, we should regard effects of viral charges on steam sheet holes and spinors. We can obtain the below frequency:

$$\begin{aligned}
V_{induced\ Virus} &= \frac{1}{2\pi} \left[\frac{K_{Steam}}{M_{electron}} \right]^{\frac{1}{2}} \rightarrow \frac{1}{2\pi} \odot \left[[\Sigma_j n_{sheet, j} \Sigma_i n_{bubble, ij} [\Sigma_k n_{\uparrow\uparrow, ijk} \right. \\
& \odot [m_{\uparrow\uparrow, ijk} - m_{radiated}(\uparrow\uparrow), (virus-cell), ijk] + m_{radiated}(\uparrow\uparrow), induced\ Virus, ijk] + \Sigma_l n_{\downarrow\downarrow, ijl} \\
& \odot [m_{\downarrow\downarrow, ijl} - m_{radiated}(\downarrow\downarrow), (virus-cell), ijl] + m_{radiated}(\downarrow\downarrow), induced\ Virus, ijl]] \\
& + [\Sigma_m n_{sheet, m} \Sigma_n n_{bubble, mn} [\Sigma_x n_{\uparrow\uparrow, mnx} \\
& \odot [m'_{\uparrow\uparrow, mnx} - m'_{radiated}(\uparrow\uparrow), (virus-cell), mnx] + m'_{radiated}(\uparrow\uparrow), induced\ Virus, mnx] + \Sigma_y n_{\downarrow\downarrow, mny} \\
& \odot [m'_{\downarrow\downarrow, mny} - m'_{radiated}(\downarrow\downarrow), (virus-cell), mny] + m'_{radiated}(\downarrow\downarrow), induced\ Virus, mny]]] + m_{noise} \Big]^{-\frac{1}{2}} \\
& \odot \left[[2\pi [\Sigma_j n_{sheet, j} \Sigma_i n_{bubble, ij}] [\Sigma_j n_{sheet, j}] + 2\pi [\Sigma_m n_{sheet, m} \Sigma_i n_{bubble, mn}] [\Sigma_m n_{sheet, m}] \right]
\end{aligned}$$

$$\begin{aligned}
& \frac{\odot [\mathcal{N}'\hbar]^2}{2\mu_0} [\Sigma_j n_{sheet}, j \Sigma_i n_{bubble}, ij [\Sigma_k [n_{\uparrow\uparrow}, ijk S_{\uparrow\uparrow}, ijk - n_{radiated}(\uparrow\uparrow), (virus-cell), ijk S_{radiated}(\uparrow\uparrow), (virus-cell), ijk \\
& + n_{radiated}(\uparrow\uparrow), induced\ Virus, ijk S_{radiated}(\uparrow\uparrow), induced\ Virus, ijk] + \Sigma_l [n_{\downarrow\downarrow}, ijl S_{\downarrow\downarrow}, ijl \\
& - n_{radiated}(\downarrow\downarrow), (virus-cell), ijl S_{radiated}(\downarrow\downarrow), (virus-cell), ijl \\
& + n_{radiated}(\downarrow\downarrow), induced\ Virus, ijl S_{radiated}(\downarrow\downarrow), induced\ Virus, ijl]]] \odot \left[\prod_{z=1 \dots n} \cos \alpha_{1, noise} \dots \cos \alpha_{w, noise} \right] \times \\
& \odot [\Sigma_{f_1=0, 1} \tan^{f_1} \alpha_{1, noise}] \dots [\Sigma_{f=0, 1} \tan^f \alpha_{w, noise}] \frac{\odot [\mathcal{N}'\hbar]^2}{2\mu_0} [\Sigma_m n_{sheet}, m \Sigma_n n_{bubble}, mn \\
& \odot [\Sigma_x [n_{\uparrow\uparrow}, mnx S'_{\uparrow\uparrow}, mnx - n_{radiated}(\uparrow\uparrow), (virus-cell), mnx S'_{radiated}(\uparrow\uparrow), (virus-cell), mnx \\
& + n_{radiated}(\uparrow\uparrow), induced\ Virus, mnx S'_{radiated}(\uparrow\uparrow), induced\ Virus, mnx] + \Sigma_y [n_{\downarrow\downarrow}, mny S'_{\downarrow\downarrow}, mny \\
& - n_{radiated}(\downarrow\downarrow), (virus-cell), mny S'_{radiated}(\downarrow\downarrow), (virus-cell), mny \\
& + n_{radiated}(\downarrow\downarrow), induced\ Virus, mny S'_{radiated}(\downarrow\downarrow), induced\ Virus, mny]]] \odot [H_{Separation\ Distance}]^{1/2} \tag{22}
\end{aligned}$$

where $v_{induced\ Virus}$ is the frequency of waves which induced virtual viruses around cells. Also, $M_{electron}$ is the mass of electron and k_{steam} is a constant related to force which acts on the steam planes of bubbles. Waves with this frequencies are able to induce virtual viruses around (virus-cell) systems. These virtual viruses interact with real viruses and reduce their effects. This frequency cause to motions of charges and their velocity which could be obtained from below equation:

$$\begin{aligned}
V_{virus-cell, bubbles} = & L_{sheet-sheet} [2\pi v_{induced\ Virus}]_{sheet-sheet} [[\Sigma_j n_{sheet}, j \Sigma_i n_{bubble}, ij [\Sigma_k n_{\uparrow\uparrow}, ijk \\
& \odot [m_{\uparrow\uparrow}, ijk - m_{radiated}(\uparrow\uparrow), (virus-cell), ijk + m_{radiated}(\uparrow\uparrow), induced\ Virus, ijk] + \Sigma_l n_{\downarrow\downarrow}, ijl \\
& \odot [m_{\downarrow\downarrow}, ijl - m_{radiated}(\downarrow\downarrow), (virus-cell), ijl + m_{radiated}(\downarrow\downarrow), induced\ Virus, ijl]]] \\
& + [\Sigma_m n_{sheet}, m \Sigma_n n_{bubble}, mn [\Sigma_x n_{\uparrow\uparrow}, mnx \\
& \odot [m'_{\uparrow\uparrow}, mnx - m'_{radiated}(\uparrow\uparrow), (virus-cell), mnx + m'_{radiated}(\uparrow\uparrow), induced\ Virus, mnx] + \Sigma_y n_{\downarrow\downarrow}, mny
\end{aligned}$$

$$\begin{aligned}
& \odot [m'_{\downarrow\downarrow, mny} - m'_{\text{radiated}(\downarrow\downarrow), (\text{virus-cell}), mny} + m'_{\text{radiated}(\downarrow\downarrow), \text{induced Virus}, mny}]] + m_{\text{noise}}]^{-\frac{1}{2}} \\
& \odot [[2\pi[\Sigma_j n_{\text{sheet}, j} \Sigma_i n_{\text{bubble}, ij}] [\Sigma_j n_{\text{sheet}, j}] + 2\pi[\Sigma_m n_{\text{sheet}, m} \Sigma_i n_{\text{bubble}, nm}] [\Sigma_m n_{\text{sheet}, m}]] \\
& \frac{\odot [\mathcal{N}' \hbar]^2}{2\mu_0} [\Sigma_j n_{\text{sheet}, j} \Sigma_i n_{\text{bubble}, ij} [\Sigma_k [n_{\uparrow\uparrow, ijk} S_{\uparrow\uparrow, ijk} - n_{\text{radiated}(\uparrow\uparrow), (\text{virus-cell}), ijk} S_{\text{radiated}(\uparrow\uparrow), (\text{virus-cell}), ijk} \\
& + n_{\text{radiated}(\uparrow\uparrow), \text{induced Virus}, ijk} S_{\text{radiated}(\uparrow\uparrow), \text{induced Virus}, ijk}] + \Sigma_l [n_{\downarrow\downarrow, ijl} S_{\downarrow\downarrow, ijl} \\
& - n_{\text{radiated}(\downarrow\downarrow), (\text{virus picell}), ijl} S_{\text{radiated}(\downarrow\downarrow), (\text{virus picell}), ijl} \\
& + n_{\text{radiated}(\downarrow\downarrow), \text{induced Virus}, ijl} S_{\text{radiated}(\downarrow\downarrow), \text{induced Virus}, ijl}]] \\
& \odot [\prod_{z=1 \dots n} \cos \alpha_{1, \text{noise}} \dots \cos \alpha_{w, \text{noise}}] \times \odot [\Sigma_{f_1=0, 1} \tan^{f_1} \alpha_{1, \text{noise}}] \dots [\Sigma_{f=0, 1} \tan^f \alpha_{w, \text{noise}}] \\
& \frac{\odot [\mathcal{N}' \hbar]^2}{2\mu_0} [\Sigma_m n_{\text{sheet}, m} \Sigma_n n_{\text{bubble}, mn} \\
& \odot [\Sigma_x [n_{\uparrow\uparrow, mnx} S'_{\uparrow\uparrow, mnx} - n_{\text{radiated}(\uparrow\uparrow), (\text{virus-cell}), mnx} S'_{\text{radiated}(\uparrow\uparrow), (\text{virus-cell}), mnx} \\
& + n_{\text{radiated}(\uparrow\uparrow), \text{induced Virus}, mnx} S'_{\text{radiated}(\uparrow\uparrow), \text{induced Virus}, mnx}] \\
& + \Sigma_y [n_{\downarrow\downarrow, mny} S'_{\downarrow\downarrow, mny} - n_{\text{radiated}(\downarrow\downarrow), (\text{virus-cell}), mny} S'_{\text{radiated}(\downarrow\downarrow), (\text{virus-cell}), mny} \\
& + n_{\text{radiated}(\downarrow\downarrow), \text{induced Virus}, mny} S'_{\text{radiated}(\downarrow\downarrow), \text{induced Virus}, mny}]] \odot H_{\text{Separation Distance}}]^{1/2} \tag{23}
\end{aligned}$$

From other side, total charges which move by this wave could be obtained from below equation:

$$\begin{aligned}
Q_{\text{virus-cell, bubbles}} = & [[\Sigma_j n_{\text{sheet}, j} \Sigma_i n_{\text{bubble}, ij} [\Sigma_k n_{\uparrow\uparrow, ijk} \\
& \odot [Q_{\uparrow\uparrow, ijk} - Q_{\text{radiated}(\uparrow\uparrow), (\text{virus-cell}), ijk} + Q_{\text{radiated}(\uparrow\uparrow), \text{induced Virus}, ijk}] + \Sigma_l n_{\downarrow\downarrow, ijl} \\
& \odot [Q_{\downarrow\downarrow, ijl} - Q_{\text{radiated}(\downarrow\downarrow), (\text{virus-cell}), ijl} + Q_{\text{radiated}(\downarrow\downarrow), \text{induced Virus}, ijl}]]
\end{aligned}$$

$$\begin{aligned}
& + [\Sigma_m n_{sheet}, m \Sigma_n n_{bubble}, mn [\Sigma_x n_{\uparrow\uparrow}, mnx \\
& \odot [Q'_{\uparrow\uparrow}, mnx - Q'_{radiated} (\uparrow\uparrow), (virus-cell), mnx + Q'_{radiated} (\uparrow\uparrow), induced\ Virus, mnx] + \Sigma_y n_{\downarrow\downarrow}, mny \\
& \odot [Q'_{\downarrow\downarrow}, mny - Q'_{radiated} (\downarrow\downarrow), (virus-cell), mny + Q'_{radiated} (\downarrow\downarrow), induced\ Virus, mny]]] + Q_{noise}
\end{aligned} \tag{24}$$

Using Equations (23) and (24), we obtain the below current density:

$$\begin{aligned}
J_{virus-cell, bubbles} \rightarrow Q_{virus-cell, bubbles} V_{virus-cell, bubbles} \rightarrow \\
& [[\Sigma_j n_{sheet}, j \Sigma_i n_{bubble}, ij [\Sigma_k n_{\uparrow\uparrow}, ijk \\
& \odot [Q_{\uparrow\uparrow}, ijk - Q_{radiated} (\uparrow\uparrow), (virus-cell), ijk + Q_{radiated} (\uparrow\uparrow), induced\ Virus, ijk] \Sigma_l n_{\downarrow\downarrow}, ijl \\
& \odot [Q_{\downarrow\downarrow}, ijl - Q_{radiated} (\downarrow\downarrow), (virus-cell), ijl + Q_{radiated} (\downarrow\downarrow), induced\ Virus, ijl]]] \\
& + [\Sigma_m n_{sheet}, m \Sigma_n n_{bubble}, mn [\Sigma_x n_{\uparrow\uparrow}, mnx \\
& \odot [Q'_{\uparrow\uparrow}, mnx - Q'_{radiated} (\uparrow\uparrow), (virus-cell), mnx + Q'_{radiated} (\uparrow\uparrow), induced\ Virus, mnx] + \Sigma_y n_{\downarrow\downarrow}, mny \\
& \odot [Q'_{\downarrow\downarrow}, mny - Q'_{radiated} (\downarrow\downarrow), (virus-cell), mny + Q'_{radiated} (\downarrow\downarrow), induced\ Virus, mny]]] + Q_{noise} \\
& \odot [L_{sheet-sheet} [[\Sigma_j n_{sheet}, j \Sigma_i n_{bubble}, ij [\Sigma_k n_{\uparrow\uparrow}, ijk \\
& \odot [m_{\uparrow\uparrow}, ijk - m_{radiated} (\uparrow\uparrow), (virus-cell), ijk + m_{radiated} (\uparrow\uparrow), induced\ Virus, ijk] + \Sigma_l n_{\downarrow\downarrow}, ijl \\
& \odot [m_{\downarrow\downarrow}, ijl - m_{radiated} (\downarrow\downarrow), (virus-cell), ijl + m_{radiated} (\downarrow\downarrow), induced\ Virus, ijl]]] + [\Sigma_m n_{sheet}, m \Sigma_n n_{bubble}, mn [\Sigma_x n_{\uparrow\uparrow}, mnx \\
& \odot [m'_{\uparrow\uparrow}, mnx - m'_{radiated} (\uparrow\uparrow), (virus-cell), mnx + m'_{radiated} (\uparrow\uparrow), induced\ Virus, mnx] + \Sigma_y n_{\downarrow\downarrow}, mny \\
& \odot [m'_{\downarrow\downarrow}, mny - m'_{radiated} (\downarrow\downarrow), (virus-cell), mny + m'_{radiated} (\downarrow\downarrow), induced\ Virus, mny]]] + m_{noise}]^{-\frac{1}{2}} \\
& \odot [[2\pi [\Sigma_j n_{sheet}, j \Sigma_i n_{bubble}, ij] [\Sigma_j n_{sheet}, j] + 2\pi [\Sigma_m n_{sheet}, m \Sigma_i n_{bubble}, mn] [\Sigma_m n_{sheet}, m]]
\end{aligned}$$

$$\begin{aligned}
& \frac{\odot[\mathcal{N}'\hbar]^2}{2\mu_0} [\Sigma_j n_{sheet, j} \Sigma_i n_{bubble, ij} [\Sigma_k [n_{\uparrow\uparrow, ijk} S_{\uparrow\uparrow, ijk} - n_{radiated(\uparrow\uparrow), (virus-cell), ijk} S_{radiated(\uparrow\uparrow), (virus-cell), ijk} \\
& + n_{radiated(\uparrow\uparrow), induced\ Virus, ijk} S_{radiated(\uparrow\uparrow), induced\ Virus, ijk}] + \Sigma_l [n_{\downarrow\downarrow, ijl} S_{\downarrow\downarrow, ijl} \\
& - n_{radiated(\downarrow\downarrow), (virus-cell), ijl} S_{radiated(\downarrow\downarrow), (virus-cell), ijl} + n_{radiated(\downarrow\downarrow), induced\ Virus, ijl} S_{radiated(\downarrow\downarrow), induced\ Virus, ijl}]] \\
& \odot [\prod_{z=1\dots n} \cos \alpha_{1, noise} \dots \cos \alpha_{w, noise}] \times \odot [\Sigma_{f_1=0, 1} \tan^{f_1} \alpha_{1, noise}] \dots [\Sigma_{f_w=0, 1} \tan^{f_w} \alpha_{w, noise}] \\
& \frac{\odot[\mathcal{N}'\hbar]^2}{2\mu_0} [\Sigma_m n_{sheet, m} \Sigma_n n_{bubble, mn} \odot [\Sigma_x [n_{\uparrow\uparrow, mnx} S'_{\uparrow\uparrow, mnx} \\
& - n_{radiated(\uparrow\uparrow), (virus-cell), mnx} S'_{radiated(\uparrow\uparrow), (virus-cell), mnx} + n_{radiated(\uparrow\uparrow), induced\ Virus, mnx} S'_{radiated(\uparrow\uparrow), induced\ Virus, mnx}] \\
& + \Sigma_y [n_{\downarrow\downarrow, mny} S'_{\downarrow\downarrow, mny} - n_{radiated(\downarrow\downarrow), (virus-cell), mny} S'_{radiated(\downarrow\downarrow), (virus-cell), mny} \\
& + n_{radiated(\downarrow\downarrow), induced\ Virus, mny} S'_{radiated(\downarrow\downarrow), induced\ Virus, mny}]] \odot [H_{Separation\ Distance}]^{1/2} \quad (25)
\end{aligned}$$

Above equation shows the current of bubbles which produce virtual Viruses around (virus-cell)s. These viruses make some virtual connections with real viruses. These real viruses make a mistake in diagnosing other real viruses and connect with virtual viruses which have opposite spins. Consequently, real-virtual viral systems become spinless and viral effects disappear.

4. Discussions

Up to date, several medical methods have been proposed to cure COVID-19; however, some of these techniques are very expensive for non-developing countries. For this reason, it is needed to employ newest scientific techniques which be more cheapest. In this research, we suggest a spinor medical method in controlling this disease. In this model, we will use of spinning oxygen molecules to cancel harmful effects of spinning viruses. To open discussion, we should remember that SARS-COV2 causes to a decrease in needed oxygen molecules within the lung. There are several reasons for this event, however, we propose a new evidence which may be ignored. We suppose that hemoglobin molecules which contain iron atoms move along blood vessels around alveolus of lungs and change spins of ions, charges and biological molecules within or around alveolar cells. These spinning cells attract triplet oxygen molecules with opposite spins. For example, a cell with $(\downarrow\downarrow \dots)$ spins attract oxygen molecule with opposite spins $(O-O(\uparrow\uparrow))$. The same may occur for spinning viruses. Alveolar spinning cells (for example with $\downarrow\downarrow \dots$) select spinning viruses with opposite spins $(\uparrow\uparrow \dots)$. On the other hand, these viruses could repel oxygen molecules with the parallel spins and cause to a decrease in needed oxygen for human's body. In this hypothesis, spins of biological cells for any person at each time may be different. To cure spinning viral diseases, we can design a system from two connected vessels, one including water and oxygen molecules and other including viruses. Two sides of vessels are warm and their middles are cooled. We connect them to each other and close the vessel of viruses but open vessel of water molecules. During respirations, spinning oxygen and other molecules which come out of alveolus, interact with vessels and cause that anti-parallel spinors, oxygen molecules and viruses become

close and parallel spins go away. These interactions cause that molecules move along vessels and some waves exchange between them. These spinor waves induce shape of spinning viruses within water and gas vessel and produce virtual viruses. These virtual viruses could be confined by water molecules, make some bubbles and go out from system. These bubbles move towards the face, enter into the lung and alveolus and interact with real viruses. Spins of these bubbles are in opposite with spins of real viruses and absorb them. Consequently, some spinless bubbles are emerged which have no effect on cells. This model could be used also in building spinor masks. These masks are formed from viruses, water and oxygen molecules. During respirations, spinning oxygen molecules which go out of alveolus, change the spins of molecules within the mask. Consequently, spinning viruses which could be selected by alveolar cells go away from the face and become close to other end of mask. These viruses repel similar spinning viruses and prevent of their absorbing by mouth and nose.

5. Conclusions

One of main problems which occur during COVID-19 disease is decreasing of needed oxygen molecules within the human's lungs. This may have many parallel reasons for example, applying oxygen molecules in building biological objects by cells or viruses. However, besides these reasons, one may guess that spinor interactions between viruses and oxygen triplets cause to repels of oxygen molecules and their reductions. Oxygen molecules have triplet states which means at least two spins of them are parallel to each other ($O-O(\uparrow\uparrow)$). On the other hand, viruses are built from many charges like electrons which have spins and it is natural that some viruses have special spins in some conditions. These spinning viruses could repel oxygen and other biological molecules with the same spins and attract any anti-parallel spinor. For example, spinors within alveolar cells of lungs are connected to blood molecules and hemoglobins and could take some spinning states from iron atoms within them. These spinors attract oxygen molecules and spinning viruses with opposite spins and repel similar spins. With respect to this point that spinors of viruses may be very more than oxygen molecules, these particles remain within the alveolus and oxygen molecules go out. We can use of these molecules in diagnosing selected spins by alveolar cells. We could put two connected vessels, one opens and includes water and oxygen molecules and other one is closed and includes viruses. We change temperature along this system from warm to cool and then warm again. During respirations, spinning molecules interact with molecules in this system and similar spinning molecules and viruses go away and anti-parallel spinors become close to the face. By changing temperature, some spinor waves are exchanged between two vessels and some virtual spinning viruses are produced and confined within the water bubbles. These bubbles go out of open vessels and move towards the face. These bubbles could enter into alveolus and interact with real viruses. Spins of bubbles and real viruses are opposite and interact each other. Consequently, some spinless bubbles are emerged which have no effects on alveolar cells. One can use of this technique in designing a spinor mask. This mask contains water and oxygen molecules and viruses. During respirations, non-effective viruses become close to the face and effective viruses go away and located on other side. These spinning viruses repel similar harmful viruses and prevent of their closing to the face. We formulated the model and obtained the currents of bubbles and oxygen molecules and also frequencies of needed waves for inducing virtual viruses around real viruses within lung.

Conflict of interest

The authors declare no competing financial interest.

References

- [1] Andersen KG, Rambaut A, Lipkin WI, Holmes EC, Garry RF. The proximal origin of SARS-CoV-2. *Nature Medicine*. 2020; 26(4): 450-452.

- [2] Wu X, Nethery RC, Sabath MB, Braun D, Dominici F. Air pollution and COVID-19 mortality in the united states: strengths and limitations of an ecological regression analysis. *Science Advances*. 2020; 6(45): eabd4049.
- [3] Wang CC, Prather KA, Sznitman J, Jimenez JL, Lakdawala SS, Tufekci Z, et al. Airborne transmission of respiratory viruses. *Science*. 2021; 373(6558): eabd9149.
- [4] Yang W, Kandula S, Huynh M, Greene SK, Van Wye G, Li W, et al. Estimating the infection-fatality risk of SARS-CoV-2 in New York City during the spring 2020 pandemic wave: a model-based analysis. *The Lancet Infectious Diseases*. 2021; 21(2): 203-212.
- [5] Krammer F. SARS-CoV-2 vaccines in development. *Nature*. 2020; 586(7830): 516-527.
- [6] Kowalski PS, Rudra A, Miao L, Anderson DG. Delivering the messenger: Advances in technologies for therapeutic mRNA delivery. *Molecular Therapy*. 2019; 27(4): 710-728.
- [7] Verbeke R, Lentacker I, De Smedt SC, Dewitte H. Three decades of messenger RNA vaccine development. *Nano Today*. 2019; 28: 100766.
- [8] Wu S, Zhong G, Zhang J, Shuai L, Zhang Z, Wen Z, et al. A single dose of an adenovirus-vectored vaccine provides protection against SARS-CoV-2 challenge. *Nature Communications*. 2020; 11(1): 4081.
- [9] Petrovsky N, Aguilar JC. Vaccine adjuvants: current state and future trends. *Immunology and Cell Biology*. 2004; 82(5): 488-496.
- [10] Cully M. A tale of two antiviral targets-and the COVID-19 drugs that bind them. *Nature Reviews Drug Discovery*. 2021; 21(1): 3-5.
- [11] Vandyck K, Deval J. Considerations for the discovery and development of 3-chymotrypsin-like cysteine protease inhibitors targeting SARS-CoV-2 infection. *Current Opinion in Virology*. 2021; 49: 36-40.
- [12] Hurt AC, Wheatley AK. Neutralizing antibody therapeutics for COVID-19. *Viruses*. 2021; 13(4): 628.
- [13] Tabish TA, Hamblin MR. Multivalent nanomedicines to treat COVID-19: A slow train coming. *Nano Today*. 2020; 35: 100962.
- [14] Tabish T, Narayan R, Edirisinghe M. Rapid and label-free detection of COVID-19 using coherent anti-Stokes Raman scattering microscopy. *MRS Communications*. 2020; 10(4): 566-572.
- [15] Logeswari K, Ravichandran C, Nisar KS. Mathematical model for spreading of COVID-19 virus with the Mittag-Leffler kernel. *Numerical Methods for Partial Differential Equations*. 2020; 40(1): e22652.
- [16] Maji C, Al Basir F, Mukherjee D, Nisar K, Ravichandran C. COVID-19 propagation and the usefulness of awareness-based control measures: A mathematical model with delay. *AIMS Mathematics*. 2022; 7(7): 12091-12105.
- [17] Vijayaraj V, Ravichandran C, Nisar KS, Valliammal N, Logeswari K, Albalawi W, et al. An outlook on the controllability of non-instantaneous impulsive neutral fractional nonlocal systems via Atangana-Baleanu-Caputo derivative. *Arab Journal of Basic and Applied Sciences*. 2023; 30(1): 440-451.
- [18] Jothimani K, Valliammal N, Alsaeed S, Nisar KS, Ravichandran C. Controllability results of hilfer fractional derivative through integral contractors. *Quality Theory Dynamics Systems*. 2023; 22: 137.
- [19] Nisar KS, Logeswari K, Ravichandran C, Sabarinathan S. New frame of fractional neutral ABC-derivative with IBC and mixed delay. *Chaos, Solitons & Fractals*. 2023; 175(Part 2): 114050.
- [20] Rehman AU, Singh R, Agarwal P. Modeling, analysis and prediction of new variants of COVID-19 and dengue co-infection on complex network. *Chaos, Solitons & Fractals*. 2021; 150: 111008.
- [21] Singh R, Tiwari P, Band SS, Rehman AU, Mahajan S, Ding Y, et al. Impact of quarantine on fractional order dynamical model of COVID-19. *Computational Biology and Medicine*. 2022; 151(Pt A): 106266.